CHEMPHYSCHEM

DOI: 10.1002/cphc.200700390

Hierarchical Structure-Within-Structure Morphologies in A_2-*star*-(B-*alt*-C) Molecules

Ching-I Huang* and Chih-Ming Chen[a]

We employ dissipative particle dynamics (DPD) to examine the self-assembly behavior of A_2-star-(B-alt-C) molecules. We successfully observe various types of hierarchical structure-within-structures, such as A-formed spheres in the matrix formed by B and C alternating layers, hexagonally packed A-formed cylinders in the matrix with B and C segregated layers, B and C alternating layers-within-lamellae, coaxial B and C alternating domains within hexagonally packed BC-formed cylinders in the A-matrix, and co-centric BC-alternating domains within BC-formed spheres in the A-matrix, by increasing the A composition. Generally speaking, the small length-scale B and C segregated domains are in parallel to the large length-scale structures. This hierarchical periodicity along the same axis as well as the various characteristic structures, that the A_2-star-(B-alt-C) copolymers display, are quite different from those in A-block-(B-graft-C) coil-comb copolymers. Moreover, it is interesting to find that when the copolymer chain length increases, though the hierarchical structure type is maintained, the number of small length-scale lamellae that can form within the large length-scale structure increases. These hierarchical structures under various compositions are reported theoretically for the first time in the copolymer systems consisting of the alternating blocks, and are in good agreement with the most recent experimental work by Matsushita and coworkers (Macromolecules ***2007***, 40, *4023*).

1. Introduction

With the improvement in synthetic techniques, copolymers with more complex forms of molecular architectures or with more than two types of monomers have been successfully formulated. These copolymers possess more diverse microstructures, which impose different influences upon various properties of polymers. Recently, copolymers with hierarchical structures have received high degrees of attention due to their potential applications as electrical, optical and other functional materials.[1–4]

Generally speaking, when the incompatibility degree between A and B is significant, traditional AB linear diblock copolymers form microphase-separated structures at only one characteristic length-scale usually within 10–100 nm range. The morphology type is mainly dominated by the composition. For instance, a series of microstructures such as A-formed spheres (S_A), hexagonally-packed A-formed cylinders (C_A^{HEX}), gyroid of minority A (G_A), lamellae (L), gyroid of minority B (G_B), hexagonally-packed B-formed cylinders (C_B^{HEX}), and B-formed spheres (S_B), is expected upon increasing the A composition f_A.[5] When a third monomer type C is involved, copolymers often exhibit two length-scale hierarchical structure-within-structure morphologies. Current research has mostly focused on the A-*block*-(B-*graft*-C) coil-comb copolymers.[2–4,6–13] There, the large length-scale ordering morphology is mainly driven by the segregation between the A-coil blocks and the BC-comb blocks, and hence depends on the block composition. Once the interaction parameter between B and C becomes significantly large, small length-scale lamellar ordering of B and C segregation, which typically ranges between 1–10 nm, frequently occurs within the original BC-rich domains. For instance, Ikkala and ten Brinke and co-workers synthesized a series of polystyrene-*block*-poly (4-vinylpyridine) (PS-*block*-P4VP) copolymers with pentadecylphenol (PDP) as side chains, which are grafted into the P4VP blocks through hydrogen bonds.[2,3,6,13] The resulting coil-comb copolymers, examined by transmission electron microscopy (TEM) and small angle X-ray scattering (SAXS), display a variety of hierarchical structures with two different length scales at room temperature, such as spherical-within-lamellar, cylindrical-within-lamellar, gyroid-within-lamellar, lamellar-within-lamellar, lamellar-within-cylindrical, and lamellar-within-spherical. Similarly, Tsao and Chen also observed the formation of structure-within-structure in poly(1,4-butadiene)-*block*-poly(ethylene oxide) (PB-*block*-PEO) with dodecylbenzenesulfonic acid (DBSA) attached to PEO through hydrogen bonds.[9] In addition, they reported that a large-scale morphology transition can be driven by the small length-scale transition concurrently in this PB-*block*-(PEO-*graft*-DBSA) copolymer.

In fact, coil-comb copolymers are not the only ones that can form hierarchical structures. By substituting the B-*graft*-C comb block with BC-alternating (denoted as B-*alt*-C) block, it is also possible to generate the small length-scale structures within the large scale domains. Typical examples are copolymers containing a linear A-homopolymer block and a BC-alternating block with linear and simple graft (i.e. three-arm star) architectures, which are referred to as A-*block*-(B-*alt*-C) and A_2-*star*-(B-*alt*-C), respectively. To our knowledge, there exist only a few

[a] *Prof. C.-I. Huang, C.-M. Chen*
Institute of Polymer Science and Engineering
National Taiwan University
Taipei 106 (Taiwan)
Fax: (+886) 2-33665237
E-mail: chingih@ntu.edu.tw

relevant studies, which have addressed the formation of two length-scale hierarchical structures on the multiblock copolymer with two or three chemically different monomers but different block lengths.[14–20] Theoretically, Nap and co-workers employed self-consistent mean-field (SCMF) theory to examine the phase behavior of A-*block*-(B-*alt*-A) copolymers.[14] They reported that when the A-coil block length is short, the systems tend to form small length-scale segregation between the alternating A and B blocks, in which the A-coil block resides inside the A-rich domains formed by the alternating A blocks. In contrast, a large length-scale diblock-like separation between the A-coil blocks and B-*alt*-A blocks frequently occurs when the A-coil is long. If both blocks have comparable lengths, coexistence of the two aforementioned length scale ordering morphology is possible.[16] Experimentally, Matsushita and co-workers were the first to observe the hierarchical lamellar-within-lamellar structure formed by styrene (*S*)-isoprene (I) undecablock copolymers, in which both S end-blocks are long and the middle S and I alternating blocks are short.[15] Later, they synthesized a new undecablock terpolymer consisting of two long poly(2-vinylpyridine) (P) end-blocks and short S and I alternating middle-blocks, and observed the formation of a highly ordered hierarchical lamellar structure including a thick P layer and five thin I-S-I-S-I layers.[18] The two-length-scale ordering lamellae formed along the same axis are different from those formed perpendicular to each other in comb-coil copolymers. This hierarchical periodicity along the same axis is a unique character for the multiblock copolymers with different block lengths, and may lead to new potential applications. In addition to lamellar-within-lamellar structure, other hierarchical structures, such as spheres-within-lamellae, cylinders-within-lamellae, coaxial cylinders, and co-centric spheres, have recently been observed experimentally by Matsushita and co-workers.[20] Though a few experimental work has successfully displayed various types of unique hierarchical structures when three chemically different species are present in the copolymer systems containing the alternating blocks, the resulting phase behavior, in particular from the composition dependence, remains unexplored from the theoretical point of view.

Herein, we thus employ the dissipative particle dynamics (DPD) simulation technique to examine the self-assembly behavior of A_2-*star*-(B-*alt*-C) molecules, in which both A arms are assumed to have equal degrees of polymerization.[21,22] Generally speaking, the DPD method simplifies a long series of molecular groups into a few bead-and-spring type particles, and therefore it can simulate the molecular behavior on longer time-scales and larger length-scales compared with the classical molecular dynamics and Monte Carlo simulations. The DPD method has been successfully applied to study the mesophase behavior for a variety of amphiphilic molecule systems.[22–30] Our modeled chain, as displayed in Figure 1, consists of $2n$ beads of the B-*alt*-C block, which is grafted into the middle of the coil A block with beads equal to $2m+1$. The total number of beads for a chain is fixed at $N=(2m+1)+2n=13$, and the A composition $f_A=(2m+1)/N$ is varied. In this case, the integer m could be 1, 2, 3, 4, and 5, and the corresponding value of f_A is equal to 0.23, 0.38, 0.54, 0.69, and 0.85, respectively. In order

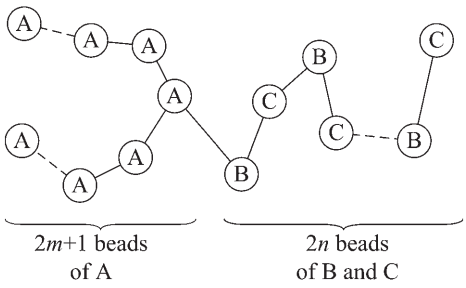

Figure 1. Schematic of A_2-*star*-(B-*alt*-C) copolymers.

to simulate the molecules with other f_A values, we adopt the same technique of blending two copolymers as has been used by Groot and Madden.[23] For example, a copolymer with $f_A=0.30$ in our case can be obtained by mixing two copolymers with $f_A=0.23$ and 0.38 at a volume ratio of 1:1. In the simulated phase behavior of AB linear diblock copolymer, Groot and Madden have shown that the mixture with a mean composition $<f_A>$ behaves as a monodisperse copolymer (i.e. with only an identical value of f_A).[23] Indeed, this is reasonable since the two blending copolymers are quite similar. Among the interaction parameters (a_{IJ}) between each pair of components I and J (where I, J = A, B, C), the interaction parameters between the A-coil block and the BC-alternating block, that is, a_{AB} and a_{AC}, play a dominant role in the large length-scale diblock-like segregation; whereas a_{BC} drives the small length-scale ordering, therefore $a_{AB}=a_{AC}$ to reduce one interaction variable. Accordingly, we aim to illustrate how the resulting morphology formation associated with two different length scales is affected by $a_{AB}=a_{AC}$, a_{BC}, and f_A.

Computational Methods

In the DPD simulation, the time evolution of motion for a set of interacting particles is solved by Newton's equation. For simplicity, we assume that the masses of all particles are equal to 1. The force acting on the *i*-th particle $\vec{f}_i$ contains three parts, a conservative force $\vec{F}_{ij}^{C}$, a dissipative force $\vec{F}_{ij}^{D}$, and a random force $\vec{F}_{ij}^{R}$: [Eq. (1)]

$$\vec{f}_i = \sum_{i \neq j} \left(\vec{F}_{ij}^{C} + \vec{F}_{ij}^{D} + \vec{F}_{ij}^{R} \right) \tag{1}$$

where the sum is over all other particles within a certain cut-off radius r_c. As this short-range cut-off counts only local interactions, r_c is usually set to 1 so that all lengths are measured relative to the particle radius. The conservative force $\vec{F}_{ij}^{C}$ is a soft repulsive force and given by Equation (2)

$$\vec{F}_{ij}^{C} = \begin{cases} a_{ij}\left(1 - \frac{r_{ij}}{r_c}\right) & r_{ij} < r_c \\ 0 & r_{ij} \geq r_c \end{cases} \tag{2}$$

where a_{ij} is the repulsive interaction parameter between particles *i* and *j*, $\vec{r}_{ij} = \vec{r}_j - \vec{r}_i$, $r_{ij} = |\vec{r}_{ij}|$, and $\vec{n}_{ij} = \frac{\vec{r}_{ij}}{r_{ij}}$. The dissipative force $\vec{F}_{ij}^{D}$ is a hydrodynamic drag force and is defined by Equation (3)

$$\vec{F}_{ij}^{D} = \begin{cases} -\gamma \omega^{D}(r_{ij})(\vec{n}_{ij} \cdot \vec{v}_{ij})\vec{n}_{ij} & r_{ij} < r_c \\ 0 & r_{ij} \geq r_c \end{cases} \tag{3}$$

where γ is a friction parameter, ω^D is a r-dependent weight function vanishing for $r \geq r_c$, and $\vec{v}_{ij} = \vec{v}_j - \vec{v}_i$. The random force $\vec{F}_{ij}^D$ corresponds to the thermal noise and has the form of Equation (4)

$$\vec{F}_{ij}^R = \begin{cases} \sigma\omega^R(r_{ij})\theta_{ij}\vec{n}_{ij} & r_{ij} < r_c \\ 0 & r_{ij} \geq r_c \end{cases} \quad (4)$$

where σ is a parameter, ω^R is a weight function, and $\theta_{ij}(t)$ is a randomly fluctuating variable. Note that these two forces $\vec{F}_{ij}^D$ and $\vec{F}_{ij}^R$ also act along the line of centers and conserve linear and angular momentum. There is an independent random function for each pair of particles. Also there is a relation between both constants γ and σ [Eq. (5)][22]

$$\sigma^2 = 2\gamma k_B T \quad (5)$$

In our simulations, $\gamma = 4.5$ and the temperature $k_BT = 1$. As such, $\sigma = 3.0$ according to Equation (5).

In order for the steady-state solution to the equation of motion to be the Gibbs ensemble and for the fluctuation-dissipation theorem to be satisfied, it has been shown that only one of the two weight functions $\omega^D$and ω^R can be chosen arbitrarily, Equation (6)[31]

$$\omega^D(r) = [\omega^R(r)]^2 \quad (6)$$

which is usually taken as Equation (7)

$$\omega^D(r) = [\omega^R(r)]^2 = \begin{cases} (r_c - r_{ij})^2 & r_{ij} < r_c \\ 0 & r_{ij} \geq r_c \end{cases} \quad (7)$$

Finally, the spring force $\vec{f}^S$, which acts between the connected beads in a molecule, has the form of Equation (8)

$$\vec{f}_i^S = \sum_j C\vec{r}_{ij} \quad (8)$$

where C is a harmonic type spring constant for the connecting pairs of beads in a molecule, and is chosen equal to 4 (in terms of k_BT).[22]

Note that a modified version of the velocity-Verlet algorithm is used here to solve the Newtonian equation of motion, [Eq. (9)][32]

$$\begin{aligned} r_i(t+\Delta t) &= r_i(t) + v_i(t)\cdot\Delta t + \frac{1}{2}f_i(t)\cdot\Delta t^2 \\ \tilde{v}_i(t+\Delta t) &= v_i(t) + \lambda f_i(t)\cdot\Delta t \\ f_i(t+\Delta t) &= f_i[r_i(t+\Delta t), \tilde{v}_i(t+\Delta t)] \\ v_i(t+\Delta t) &= v_i(t) + \frac{1}{2}\Delta t\cdot[f_i(t) + f_i(t+\Delta t)] \end{aligned} \quad (9)$$

The parameter λ is introduced to account for some additional effects of the stochastic interactions. A detailed investigation of the effects of λ on the steady-state temperature has been reported by Groot and Warren.[22] For the particle density $\rho = 3$ and the constant $\sigma = 3$, they found an optimum value of $\lambda = 0.65$, in which the temperature control can be significantly maintained even at a large time-step of 0.06. Here, we choose $\lambda = 0.65$ and the time-step $\Delta t = 0.05$ according to ref. [22].

The DPD simulations are performed in a cubic box of L^3 grids with periodic boundary conditions. The particle density ρ is set equal to 3. Hence, the total simulated DPD beads are $3L^3$. On the basis of the algorithm described above, the time evolutions of motion for these particles are started with an initially disordered configuration and simulated within the cubic box. Each simulation is performed until the formed structure remains somewhat unchanged with the time-step. In general, the resulting morphology patterns via DPD are dependent of the finite size of the simulation box, as have been reported in other theoretical studies.[33–35] In order to exclude the finite size effects, one has to keep enlarging the simulation box size until the structures are no longer affected by the simulation box. For our current model system with the total number of beads per chain $N = 13 \sim 25$, the box size ranges from $20\times20\times20$ to $30\times30\times30$. In each simulated morphology pattern, the red, green, and blue colors are used to represent A, B, and C, respectively.

2. Results and Discussion

In simulating the microphase separation behavior of A_2-*star*-(B-*alt*-C) molecules, the dimensionless interaction parameter (i.e. in terms of k_BT) between like-particles is taken as $a_{ii} = 25$ (particle density $\rho = 3$) according to the work of Groot and Warren.[22] The interaction parameter between different components i and j can be estimated by the following relationship between a_{ij} and the Flory–Huggins interaction parameter χ_{ij} derived by Groot and Warren[22] for $\rho = 3$, Equation (10)

$$a_{ij}(T) = a_{ii} + 3.497\chi_{ij}(T) \quad (10)$$

Therefore, the value of $a_{ij} \leq 25$ corresponds to $\chi_{ij} \leq 0$, which indicates that components i and j are very miscible. As the incompatibility between i and j increases, a_{ij} increases from 25.

First, we examine how the interaction parameters affect the resulting structure patterns of A_2-*star*-(B-*alt*-C) copolymers. Figure 2 displays the phase diagram in terms of a_{BC} and $a_{AB} = a_{AC}$ for the systems with $f_A = 0.54$. At a fixed value of a_{BC}, we observe that when $a_{AB} = a_{AC}$ is large enough, so that the immiscibility degree between the A-coil block and the BC-alternating block becomes significant, the molecules pack into an ordered A-rich and BC-rich segregated microstructure. Moreover, various diblock-like morphologies are induced by varying the interaction parameter a_{BC}. For instance, Figure 3 illustrates the morphology variation with a_{BC} at $a_{AB} = a_{AC} = 100$. When a_{BC} is set to be 25, both B and C are indeed indistinguishable for A since $a_{AB} = a_{AC}$ and the A_2-*star*-(B-*alt*-C) molecules are identical

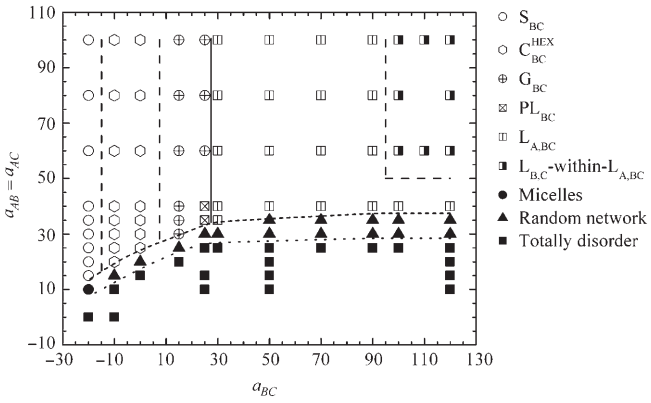

Figure 2. Phase diagram of A_2-*star*-(B-*alt*-C) copolymers in terms of the interaction parameter $a_{AB} = a_{AC}$ and a_{BC} when $f_A = 0.54$ and $N = 13$. The phase boundary lines are drawn as a guide for the eyes.

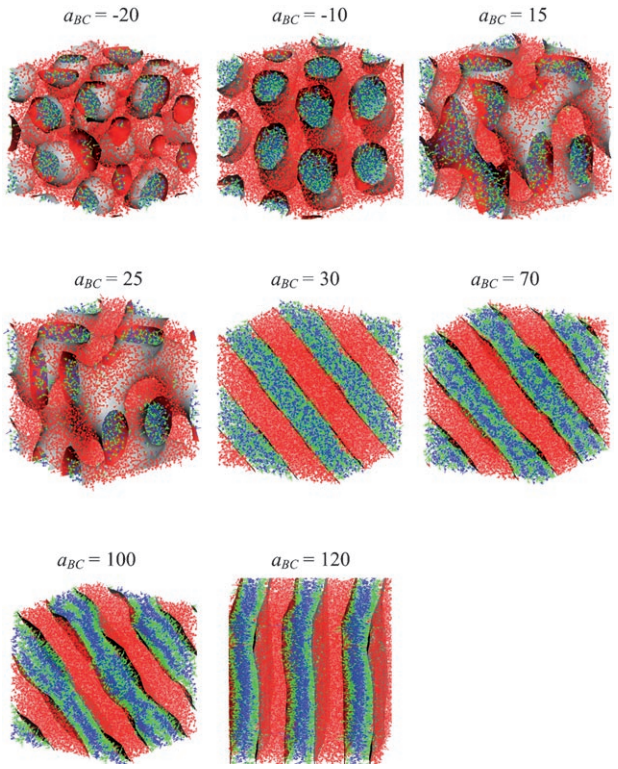

Figure 3. Morphology variation of A_2-*star*-(B-*alt*-C) copolymers with a_{BC} when $f_A = 0.54$, $N = 13$, and $a_{AB} = a_{AC} = 100$. The red, green, and blue colors represent A, B, and C, respectively. The red surface corresponds to the isosurface of component A.

to the so-called A_2B miktoarm star copolymers. Accordingly, the copolymer with $f_A = 0.54$ forms a complex gyroid phase G_{BC}, as have been predicted by self-consistent mean-field theory[36] and simulated by DPD.[30] When a_{BC} decreases from 25, due to the fact that B and C components become more attractive, the BC-alternating blocks tend to coil and transform into cylinders—and even spheres in the matrix of A-coil blocks. This transition behavior by decreasing a_{BC} is analogous to decreasing the composition of BC-alternating block. On the contrary, when a_{BC} increases from 25, one may expect that the increasing segregation degree between B and C would cause the BC-alternating chain to be more extended, and thus a transition from G_{BC} to lamellae to A-formed cylinders or spheres would occur. However, a series of the morphology variation with a_{BC}, $S_{BC}(a_{BC} = -20) \rightarrow C^{HEX}_{BC}(-10 \leq a_{BC} \leq 0) \rightarrow G_{BC}(15 \leq a_{BC} \leq 25) \rightarrow L_{A,BC}$ $(30 \leq a_{BC} \leq 90) \rightarrow L_{B,C}$-within-$L_{A,BC}(100 \leq a_{BC} \leq 120)$, is observed in Figure 3. That is, as a_{BC} increases from 25, though the segregation degree between B and C becomes more obvious, the systems still retain a stable A-rich and BC-rich lamellar phase in a wide range of a_{BC} between 30 and 90, and no further diblock-like large length-scale transition as mentioned above occurs. Indeed, these results are not surprising since when a_{BC} keeps increasing, in order to reduce the contacts between B and C, the BC-alternating chain would rather fold within the original BC-rich layers to form small length-scale B-rich and C-rich lamellae; these are the so-called hierarchical $L_{B,C}$-within-$L_{A,BC}$. Moreover, the resulting hierarchical periodicity is formed in a parallel direction to each other, which is different from that in comb-coil copolymers. When the value of $a_{AB} = a_{AC}$ is fixed to a lower value such as 40, similar morphology transitions associated with the large length-scale ordering has also been observed by varying the interaction parameter a_{BC}. Whereas, even when a_{BC} increases to a very large value of 120, we do not find the formation of the hierarchical structure-within-structure morphology induced by a_{BC}, as in the case of $a_{AB} = a_{AC}$ at larger values. Therefore in order to form the small length-scale lamellar segregation between B and C within the large-scale BC-rich domains, the interaction parameters between B and C (a_{BC}) and also between the A-coil block and the BC-alternating block (a_{AB} and a_{AC}) have to be significantly large. If the value of $a_{AB} = a_{AC}$ continues to decrease, since the repulsion between A and B(C) becomes weaker, the ordered copolymers are expected to become disordered. Note that, between the totally disordered and the well-ordered states, we observe that the systems form a micelle-like or random network structure (i.e. with chains aggregating but no formation of well-ordered structure), which we assign as the disordered phases.

Next, we discuss the phase transition behavior associated with the two length-scale ordering for A_2-*star*-(B-*alt*-C) molecules in a wide range of composition f_A. Recall that our previous results have shown that in order for a molecule with a particular value of composition f_A to form an ordered microstructure, the value of $a_{AB} = a_{AC}$ controls the order-disorder transition; while a_{BC} plays a dominant role in determining the morphology geometry at large length-scales as well as the formation of hierarchical structure-within-structure. Therefore, we fix the value of $a_{AB} = a_{AC}$ at 100, which is significant enough to assure the formation of the large length-scale diblock-like structures, and construct the corresponding phase diagram in terms of f_A and a_{BC}, as shown in Figure 4. When a_{BC} decreases from 25, it is worth noting that the regime of ordered microstructures in which the BC-blocks form the minor domains such as G_{BC}, PL_{BC}, C^{HEX}_{BC}, and S_{BC}, is enlarged noticeably and even extended to the systems with $f_A < 0.5$. For example, when $f_A = 0.3$–0.5, although the BC-block is longer than the A-block, the

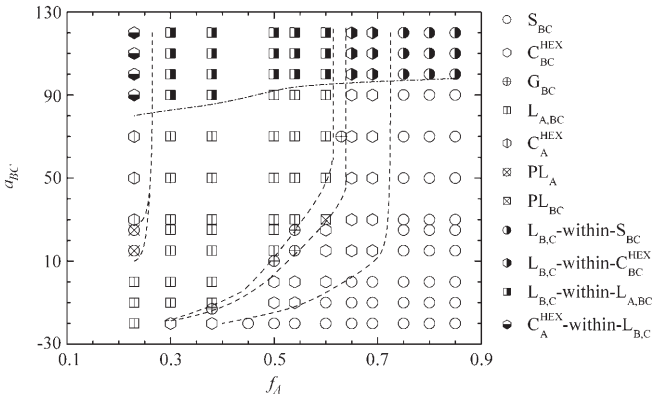

Figure 4. Phase diagram of A_2-*star*-(B-*alt*-C) copolymers with $N = 13$ in terms of the interaction parameter a_{BC} and composition f_A when $a_{AB} = a_{AC} = 100$. The phase boundary lines are drawn as a guide for the eyes.

majority BC component still tends to form the minor domains in the minority A-rich matrix; these are the so-called inverted microstructures. This is due to the fact that when B and C become more attractive, the BC-alternating blocks favor to coil together in order to reduce the contacts with the A-blocks. Note that these inverted structures have been frequently observed in block copolymer solutions by increasing the solvent selectivity and/or the solvent amount.[37,38] However, this is possibly the first study to predict their presence in the A_2-*star*-(B-*alt*-C) molecules.

Now, let us continue to discuss the phase behavior shown in Figure 4 for each molecule with a particular value of f_A when a_{BC} increases from 25. Similar to the copolymer with $f_A = 0.54$, a significant increase in the interaction parameter a_{BC} also leads to the formation of small length-scale B and C segregated lamellae within the large length-scale BC-rich domains for the copolymers with other values of f_A in the range of 0.2–0.85. In Figure 5 we display the various types of structure-within-structures, such as A-formed spheres in the matrix formed by B and C alternating layers (S_A-within-$L_{B,C}$) ($f_A \cong 0.14$), hexagonally packed A-formed cylinders in the matrix with B and C segregated layers (C_A^{HEX}-within-$L_{B,C}$) ($f_A \cong 0.23$), $L_{B,C}$-within-$L_{A,BC}$ ($0.3 \leq f_A \leq 0.6$), coaxial B and C alternating domains within hexagonally packed BC-formed cylinders in the A-matrix ($L_{B,C}$-within-C_{BC}^{HEX}) ($0.65 \leq f_A \leq 0.7$), and co-centric BC-alternating domains within BC-formed spheres in the A-matrix ($L_{B,C}$-within-S_{BC}) ($0.75 \leq f_A \leq 0.85$), which are simulated at $a_{BC} = 120$. Note that the two length-scale morphology of S_A-within-$L_{B,C}$ shown in Figure 5 is obtained for the case of N increased to 21. This is simply because of the fact that in the original case of $N = 13$, the lowest value of f_A that the system can reach is 0.23. Accordingly, in order to observe whether the S_A-within-$L_{B,C}$ structure is possible to form at smaller values of f_A, we increase N to 21. Generally speaking, the geometry of large length-scale morphology is mainly dominated by the composition f_A. This series of hierarchically ordered variation with the composition is in qualitatively good agreement with the most recent experimental work.[20] If we further examine the small length-scale formation of B and C alternating layers within the major domains, such as C_{BC}^{HEX}-within-$L_{B,C}$ and $L_{B,C}$-within-$L_{A,BC}$, it is clear that these layers are parallel to the A-formed cylinders or lamellae. More interestingly, when f_A is larger than 0.5 so that B and C segregation occurs within the minor domains such as C_{BC}^{HEX} and S_{BC}, these BC-alternating chains fold in a particular way to form multiple (more than 2) B and C coaxial cylinders or co-centric spheres. Note that when f_A is 0.85 and $N = 13$, since each molecule only contains one B and one C, we only observe C-core/B-shell spheres as in Figure 5. These multiple coaxial cylinders or co-centric spheres formed by the BC-alternating blocks in the A_2-*star*-(B-*alt*-C) copolymers are reported theoretically for the first time. Though it has been shown that the ABC linear triblock copolymers can form core-shell types of cylinders or spheres, the number of segregated layers within the domains is generally two instead of the multiple (more than two) layers that the A_2-*star*-(B-*alt*-C) can form.[39]

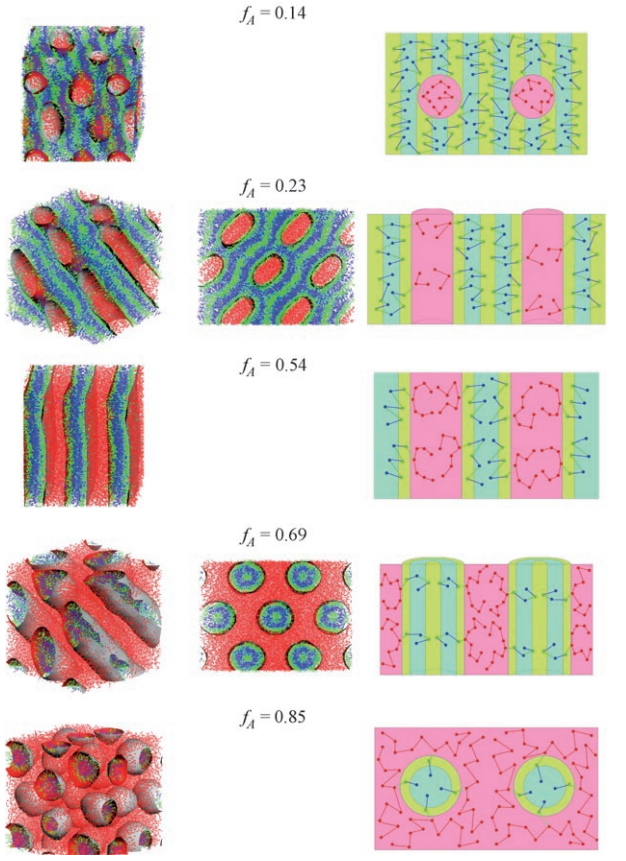

Figure 5. Morphology variation and corresponding molecular arrangements of A_2-*star*-(B-*alt*-C) copolymers ($N = 13$) with f_A when $a_{AB} = a_{AC} = 100$ and $a_{BC} = 120$. Note that the pattern when $f_A = 0.14$ corresponds to $N = 21$. The red, green, and blue colors represent A, B, and C, respectively. The red surface corresponds to the isosurface of component A.

In Figure 5, we also plot the schematic molecular alignment in detail for each structure-within-structure. Compared with the A-*block*-(B-*graft*-C) coil-comb copolymers as presented in Figure 6, we observe a completely different packing behavior of molecules due to the difference of molecular architecture. Hence, the hierarchical structure-within-structures that these two copolymers can form are significantly different. In particular, the smalllength-scale lamellae formed by the B-*alt*-C and B-*graft*-C chains display a parallel and perpendicular direction, respectively, with respect to the large length-scale structure. We believe this characteristic difference imposes different influences upon various properties of polymers, such as photoelectronic properties, and leads to different potential applications.

Finally, we address whether these characteristic structure-within-structures simulated at $N = 13$ can also be preserved when N increases. Here, we double each arm length and thus the total number of beads per chain N increases to 25. Figure 7 displays the resulting structure patterns for $N = 25$, $f_A \cong 0.54$ and 0.69, at the same interaction parameters ($a_{AB} = a_{AC} = 100$ and $a_{BC} = 120$) as in Figure 5. Note that when N increases from 13 to 25, the value of f_A should be slightly changed from 0.54 to 0.52 and 0.69 to 0.68, respectively. However, in the following comparison between both results with different N, we only denote the value of f_A for $N = 13$. When $f_A \cong 0.54$, we find that the copolymer still forms $L_{B,C}$-within-$L_{A,BC}$

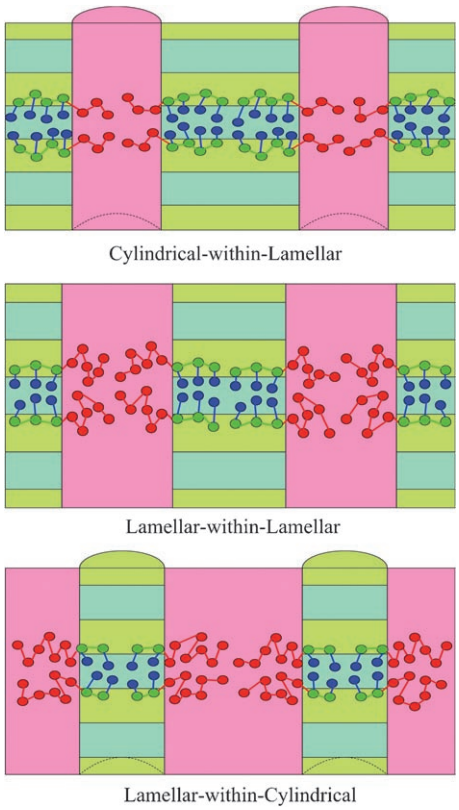

Figure 6. Schematic plot of molecular arrangements for A-*block*-(B-*graft*-C) comb-coil copolymers in various types of structure-within-structures.

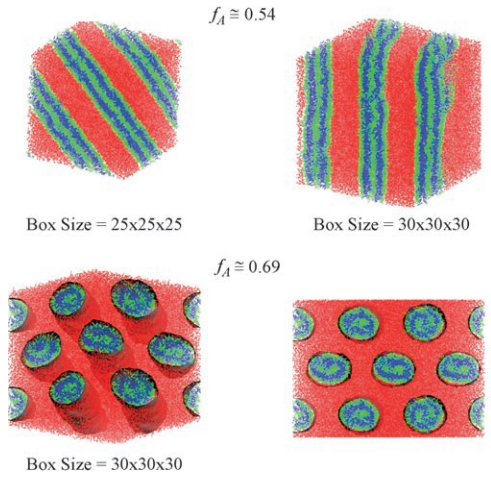

Figure 7. Structure patterns of A_2-*star*-(B-*alt*-C) copolymers with $N = 25$, $a_{AB} = a_{AC} = 100$, $a_{BC} = 120$, and f_A equal to 0.54 and 0.69, respectively. The red, green, and blue colors represent A, B, and C, respectively. The red surface corresponds to the isosurface of component A.

with increasing N from 13 (in this case, the number of BC-blocks per chain, n, is 3) to 25 ($n = 6$), but the formed B and C alternating layers within the BC-rich lamellae vary from B-C-B (three) to B-C-B-C-B (five) thin layers. This is not surprising since when N increases, more B and C segments (beads) per chain can distribute freely, and hence more sublayers within the large length-scale lamellae are possible. Recall that in the A-*block*-(B-*alt*-C)-B-*block*-A copolymers, Matsushita and co-workers predicted that the number of thin layers within the large length-scale lamellae increases from three when the number of (B-*alt*-C) per chain n equals two, to five when $3 \leq n \leq 6$, by simply comparing the numbers of possible conformations for each layered structure.[18] In addition, ten Brinke and co-workers claimed that the number of internal layers within the lamellar-in-lamellar structure formed by the same types of copolymers in the strong segregation limit is mainly dominated by the balance between the stretching of the individual blocks and the interfacial area.[19] In our DPD simulations, since we only use one bead to resemble each alternating block, the stretching effects associated with the entropy and flexibility of chains cannot be treated properly. Still, the fact that each bond between two connected beads in our model is flexible enables the chains with more B and C alternating segments to create more possible distribution ways and hence to form more internal-layered structures. To examine the number of small length-scale B and C segregated domains formed within the structure other than lamellae, we chose $f_A \cong 0.69$ and increased $N = 13$ ($n = 2$) to 25 ($n = 4$). As can be seen clearly in Figures 5 and 7, three B-C-B coaxial cylinders within C_{BC}^{HEX} are formed for both cases, although the formed cylinders for $N = 25$ are slightly elliptic. The reason that the number of B and C segregated domains in the $L_{B,C}$-within-C_{BC}^{HEX} remains constant at three when N increases from 13 to 25 may be given as follows: 1) the number of minority B and C segments per chain increases slightly ($n = 2$–4) so that the greatest number of possible chain conformations still remains and forms three-layer segregation; 2) the number of thin coaxial layers allowed to form within the cylinders is three. In order to systematically investigate this matter, a further simulation for larger N values needs to be performed in a larger simulation box, which is too time consuming and not our concern here. As far as we know, the issue that the number of allowed thin layers formed within each hierarchical structure when N becomes significantly large has not been concluded yet. However, due to the relationship between the chain-stretching energy and the interfacial energy, as proposed by ten Brinke and co-workers, it is reasonable to infer that the number of small length-scale segregated domains formed within the large length-scale structures has to reach a maximum when N keeps increasing.[19]

It should be mentioned again that since our modeled chains are indeed very short, the associated entropic effects on the resulting phase behavior of A-*block*-(B-*graft*-C) coil-comb copolymers (i.e. long chains) may not be reflected appropriately. Hence, the morphological behavior, in particular in the weak segregation regime, may differ when the chain length N increases. However, when the segregation degree becomes significantly large, so that the formation of well-ordered structures is mainly dominated by the enthalpic effects, the self-assembly behavior simulated for small values of $N = 13$ in this study should also hold true qualitatively for A_2-*star*-(B-*alt*-C) copolymers with large degrees of copolymerization N. Accordingly, our results via DPD have captured most of the important and interesting hierarchical structure-within-structures observed in the experimental work.

3. Conclusions

We employ dissipative particle dynamics to examine the phase behavior associated with two length-scale ordering of A_2-*star*-(B-*alt*-C) molecules. In particular, we assume that the interaction parameters between the coil A and the alternating B and C (a_{AB} and a_{AC}) are the same, and focus on the effects of composition f_A, and the interaction parameters a_{BC} and $a_{AB}=a_{AC}$. We successfully observe the formation of hierarchical structures with two characteristic length scales, these are the so-called structure-within-structures. In order to form the small length-scale B and C lamellar segregation within the large-scale BC-rich domains, not only a_{BC} but also a_{AB} and a_{AC} have to be significantly large. In general, the significant immiscibility between A-coil block and BC-alternating block leads to the formation of large length-scale A-rich and BC-rich morphology. In addition to the composition f_A, the interaction parameter a_{BC} has a great influence on the morphology geometry.

As a_{BC} decreases (i.e. B and C become more attractive), due to the fact that the BC-alternating blocks favor to coil together, a series of diblock-like morphology transition can be induced, which is analogous to decreasing the composition of BC-alternating block. To clarify, even when $f_A<0.5$, a decrease in a_{BC} can lead to the formation of the inverted structures, in which the major BC component forms the minor domains in the minority A-rich matrix. This is possibly the first study to predict the formation of inverted structures in the copolymer melts.

On the contrary, when a_{BC} increases so that in order to reduce the contacts between B and C, the BC-alternating chain would rather fold within the original BC-rich domains to form small length-scale B-rich and C-rich phase. Various hierarchical structures, S_A-within-$L_{B,C}$, C_A^{HEX}-within-$L_{B,C}$, $L_{B,C}$-within-$L_{A,BC}$, $L_{B,C}$-within-C_{BC}^{HEX}, and $L_{B,C}$-within-S_{BC}, are formed with an increase in f_A. It is worth noting that when B and C segregation occurs within the minor domains such as C_{BC}^{HEX} and S_{BC}, these BC-alternating chains fold in a particular way to form multiple B and C coaxial cylinders or co-centric spheres. Moreover, though the hierarchical structure type is maintained when the copolymer chain length increases, the number of small length-scale lamellae that can form within the large length-scale structure increases. Generally speaking, the small length-scale segregated domains formed by the B-*alt*-C chains are in parallel to the large length-scale structure. This hierarchical periodicity along the same axis as well as the various characteristic structures that the A_2-*star*-(B-*alt*-C) copolymers display are quite different from those in A-*block*-(B-*graft*-C) coil-comb copolymers.

Acknowledgments

This work was supported by the National Science Council of the Republic of China through grant NSC 96-2221-E-002-019.

[1] M. Muthukumar, C. K. Ober, E. L. Thomas, *Science* **1997**, *277*, 1225–1232.
[2] J. Ruokolainen, R. Makinen, M. Torkkeli, T. Makela, R. Serimaa, G. ten Brinke, O. Ikkala, *Science* **1998**, *280*, 557–560.
[3] J. Ruokolainen, G. ten Brinke, O. Ikkala, *Adv. Mater.* **1999**, *11*, 777–780.
[4] R. Maki-Ontto, K. de Moel, W. de Odorico, J. Ruokolainen, M. Stamm, G. ten Brinke, O. Ikkala, *Adv. Mater.* **2001**, *13*, 117–121.
[5] M. W. Matsen, F. S. Bates, *Macromolecules* **1996**, *29*, 1091–1098.
[6] J. Ruokolainen, M. Saariaho, O. Ikkala, G. ten Brinke, M. Torkkeli, R. Serimaa, *Macromolecules* **1999**, *32*, 1152–1158.
[7] O. Ikkala, G. ten Brinke, *Chem. Commun.* **2004**, 2131–2137.
[8] G. ten Brinke, O. Ikkala, *Chem. Rec.* **2004**, *4*, 219–230.
[9] C. S. Tsao, H. L. Chen, *Macromolecules* **2004**, *37*, 8984–8991.
[10] E. Polushkin, S. Bondzic, J. de Wit, G. Alberda van Ekenstein, I. Dolbnya, W. Bras, O. Ikkala, G. ten Brinke, *Macromolecules* **2005**, *38*, 1804–1813.
[11] A. Laiho, R. H. A. Ras, S. Valkama, J. Ruokolainen, R. Osterbacka, O. Ikkala, *Macromolecules* **2006**, *39*, 7648–7653.
[12] W. van Zoelen, G. Alberda van Ekenstein, O. Ikkala, G. ten Brinke, *Macromolecules* **2006**, *39*, 6574–6579.
[13] S. Valkama, T. Ruotsalainen, A. Nykanen, A. Laiho, H. Kosonen, G. ten Brinke, O. Ikkala, J. Ruokolainen, *Macromolecules* **2006**, *39*, 9327–9336.
[14] R. Nap, I. Erukhimovich, G. ten Brinke, *Macromolecules* **2004**, *37*, 4296–4303.
[15] Y. Nagata, J. Masuda, A. Noro, D. Cho, A. Takano, Y. Matsushita, *Macromolecules* **2005**, *38*, 10220.
[16] R. Nap, N. Sushko, I. Erukhimovich, G. ten Brinke, *Macromolecules* **2006**, *39*, 6765–6770.
[17] Y. G. Smimova, G. ten Brinke, I. Y. Erukhimovich, *J. Chem. Phys.* **2006**, *124*, 054907.
[18] J. Masuda, A. Takano, Y. Nagata, A. Noro, Y. Matsushita, *Phys. Rev. Lett.* **2006**, *97*, 098301.
[19] A. Subbotin, T. Klymko, G. ten Brinke, *Macromolecules* **2007**, *40*, 2915–2918.
[20] J. Masuda, A. Takano, J. Suzuki, Y. Nagata, A. Noro, K. Hayashida, Y. Matsushita, *Macromolecules* **2007**, *40*, 4023–4027.
[21] P. J. Hoogerbrugge, J. M. V. A. Koelman, *Europhys. Lett.* **1992**, *19*,155–160.
[22] R. D. Groot, P. B. Warren, *J. Chem. Phys.* **1997**, *107*, 4423–4435.
[23] R. D. Groot, T. J. Madden, *J. Chem. Phys.* **1998**, *108*, 8713–8724.
[24] E. Ryjkina, H. Kuhn, H. Rehage, F. Muller, J. Peggau, *Angew. Chem.* **2002**, *114*, 1025–1028; *Angew. Chem. Int. Ed.* **2002**, *41*, 983–986.
[25] S. Yamamoto, Y. Maruyama, S. Hyodo, *J. Chem. Phys.* **2002**, *116*, 5842–5849.
[26] L. Rekvig, M. Kranenburg, J. Vreede, B. Hafskjold, B. Smit, *Langmuir* **2003**, *19*, 8195–8205.
[27] H. J. Qian, Z. Y. Lu, L. J. Chen, Z. S. Li, C. C. Sun, *Macromolecules* **2005**, *38*, 1395–1401.
[28] J. Xia, C. Zhong, *Macromol. Rapid Commun.* **2006**, *27*, 1110–1114.
[29] C. I. Huang, Y. J. Chiou, Y. K. Lan, *Polymer* **2007**, *48*, 877–886.
[30] C. I. Huang, H. T. Yu, *Polymer* **2007**, *48*, 4537–4546.
[31] P. Espanol, P. B. Warren, *Europhys. Lett.* **1995**, *30*, 191–196.
[32] M. P. Allen, D. J. Tildesley, *Computer Simulation of Liquids*, Clarendon, Oxford, **1987**.
[33] U. Micka, K. Binder, *Macromol. Theory Simul.* **1995**, *4*, 419–447.
[34] Y. Bahbot-Raviv, Z. G. Wang, *Phys. Rev. Lett.* **2000**, *85*, 3428–3431.
[35] Q. Wang, P. F. Nealey, J. J. de Pablo, *Macromolecules* **2001**, *34*, 3458–3470.
[36] G. M. Grason, R. D. Kamien, *Macromolecules* **2004**, *37*, 7371–7380.
[37] C. I. Huang, T. P. Lodge, *Macromolecules* **1998**, *31*, 3556–3565.
[38] T. P. Lodge, B. Pudil, K. J. Kanley, *Macromolecules* **2002**, *35*, 4707–4717.
[39] F. S. Bates, G. H. Fredrickson, *Phys. Today* **1999**, *52*, 32–38.

Keywords: coil-alternating molecule · dissipative particle dynamics · phase transitions · self-assembly · structure elucidation

Received: June 5, 2007
Revised: September 18, 2007
Published online on October 25, 2007

